First-principles study of electronic and optical properties in wurtzite $Zn_{1-x}Cu_xO$*

Zhao Long(赵 龙), Lu Peng-Fei(芦鹏飞), Yu Zhong-Yuan(俞重远)†,
Liu Yu-Min(刘玉敏), Wang Dong-Lin(王东林), and Ye Han(叶 寒)

Key Laboratory of Information Photonics and Optical Communications (Beijing University of Posts and Telecommunications), Ministry of Education, Beijing 100876, *China*

(Received 19 July 2009; revised manuscript received 23 October 2009)

We perform a first-principles simulation to study the electronic and optical properties of wurtzite $Zn_{1-x}Cu_xO$. The simulations are based upon the Perdew–Burke–Ernzerhof form of generalised gradient approximation within the density functional theory. Calculations are carried out in different concentrations. With increasing Cu concentration, the band gap of $Zn_{1-x}Cu_xO$ decreases due to the shift of valence band. The imaginary part of the dielectric function indicates that the optical transition between O 2p states in the highest valence band and Zn 4s states in the lowest conduction band shifts to the low energy range as the Cu concentration increases. Besides, it is shown that the insertion of Cu atom leads to redshift of the optical absorption edge. Meanwhile, the optical constants of pure ZnO and $Zn_{0.75}Cu_{0.25}O$, such as loss function, refractive index and reflectivity, are discussed.

Keywords: density functional theory, Cu-doped ZnO, electronic structure, optical properties
PACC: 6185, 7125, 7115M, 7115A

1. Introduction

ZnO is a promising direct wide band-gap semiconductor. It has been extensively investigated for use in optoelectronic devices.[1−4] Typically, ZnO exhibits n-type conductivity, which has been attributed to various mechanisms including interstitial hydrogen and native defects.[5−7] The production of p-type ZnO is very difficult for its asymmetric doping limitations.[8,9] Therefore, the major bottleneck remains the fabrication of stable p-type ZnO thin films. Besides, the band gap of ZnO is too large to use visible light effectively. It is also very interesting in doping ZnO because of the possibility of tailoring its electronic structure and optical properties.[10−14]

Recent works have suggested that group-IB elements such as Cu, Ag and Au may be good candidates for producing both p-type and band-gap-reduced ZnO.[15−17] Among these three candidates, Cu could be the best choice because the size mismatch between Cu and Zn is the smallest, which leads to the lowest formation energy. Many different experimental methods have been applied to the growth of Cu-doped ZnO, such as the pulsed laser deposition (PLD) method.[17,18] Buchholz *et al.*[19] have observed room temperature ferromagnetism in Cu-doped ZnO thin films. They suggested that films grown under conditions that produce p-type semiconductor were ferromagnetic with a Curie temperature above 350 K. Ahn *et al.*[12] have reported a p-type ZnO grown by the doping with Cu ion. Theoretically, Ye *et al.*[20] have shown the ferromagnetism in Cu-doped ZnO, using the full-potential linearised augmented plane-wave method. Park and Min[21] studied electronic structures and magnetic properties of ZnO-based diluted magnetic semiconductors codoped with Fe and Cu. Chakraborti *et al.*[22] revealed that the ferromagnetism in Cu-doped ZnO films was attributed to Cu ions' substitution into the ZnO lattice.

Up to now, most of the relevant efforts have been focused on the magnetic properties of ZnO. However, the doping may also influence its electronic and optical properties. This is particularly important for future applications of ZnO in hybrid nanoelectronic, optoelectronic, and spintronic on-chip device platforms. In this paper, we present a complete simulation of Cu doping in ZnO material. The band gap and optical properties are calculated in the framework of the first principle-approach. Our simulation shows that the band structure and optical properties of ZnO is

*Project supported by the National High Technology Research and Development Program of China (Grant No. 2009AA03Z405), the National Natural Science Foundation of China (Grant Nos. 60908028 and 60971068) and the Chinese Universities Scientific Fund (Grant No. BUPT2009RC0412).
†Corresponding author. E-mail: yuzhongyuan30@gmail.com
© 2010 Chinese Physical Society and IOP Publishing Ltd

affected by the concentration of Cu. When the Cu content is larger than 25%, the band gap of ZnO will vanish.

2. Theory and computational method

2.1. Theoretical model

At ambient temperature and pressure, the stable phase of ZnO is hexagonal wurtzite structure with $P6_3mc$ space group and C_{6v}^4 symmetry. Its lattice constants are $a = b = 3.24927$ Å (1 Å = 0.1 nm), $c = 5.20544$ Å, and $c/a = 1.602$. The lattice cell of oxygen and zinc form the hexagonal close pack structure from the accumulation of reverse. All calculations are based on the supercell model, as shown in Fig. 1(a). The ligand of ZnO is a triangular cone, and the Zn–O bond length along c-axis (1.95204 Å) is shorter than that in the other directions (1.98561 Å). The 2×2×2 ZnO supercell, which contains 16 Zn and 16 O atoms, is employed. The model of Cu-doped supercell structure is shown in Fig. 1(b).

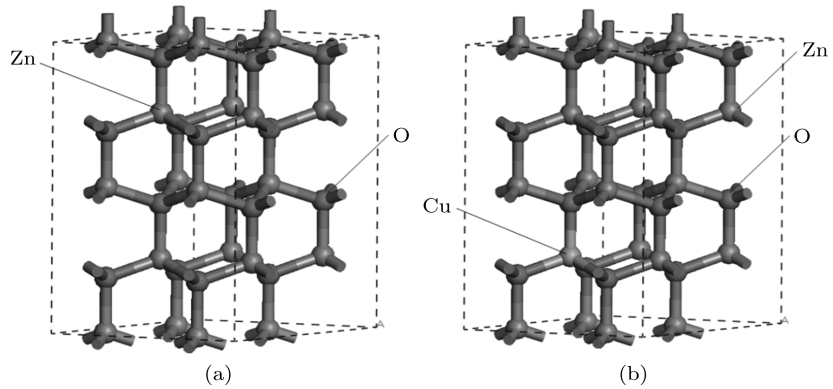


Fig. 1. (a) The supercell structure of ZnO. (b) One Zn atom is substituted by Cu atom in ZnO supercell structure.

2.2. Computational method

Our simulations are performed with the Cambridge serial total energy package (CASTEP) code, which is based on the density functional theory using a plane-wave pseudopotential method.[23] The generalised gradient approximation (GGA) in the scheme of Perdew–Burke–Ernzerhof is used to treat the exchange–correlation function,[24] since the GGA is more efficient to predict the optical transition. Meanwhile, previous studies have shown that the norm-conserving pseudopotential, which was developed by Hamann *et al.*,[25] is more suitable than the ultrasoft pseudopotential in optical properties calculations.[26] Thus, norm-conserving pseudopotential is used to describe the electron–ion interaction. Besides, the valence-electron configurations for the oxygen, zinc and copper atoms are employed as $2s^2$ $2p^4$, $3d^{10}$ $4s^2$ and $3d^{10}$ $4s^1$, respectively. The plane-wave functions of valence electrons are expanded in a plane-wave basis set. Reciprocal-space integration over the first Brillouin zone is approximated through a careful sampling at a finite number of k points using a Monkhorst–Pack mesh.[27] In our calculation, the 2×2×2 ZnO supercell consisting of 32 atoms is used and the supercell is kept at constant volume. The substitutional method has been taken into account. For $x = 0.0625$, only one Zn atom is substituted by Cu, while for $x = 0.25$, four Zn atoms are substituted. The cut-off energy has been assumed to be 460 eV according to Table 1. Meanwhile, the k-point set with parameters of 7×7×4 and 4×4×2 for pure ZnO and the ZnCuO alloys, respectively, is used over the first Brillouin zone sampling mesh. Self-consistency is considered to be achieved when the charge density difference between succeeding iterations is less than 2×10^{-6} eV/atom. The lattice constants of wurtzite ZnO are 3.24927 Å for a and 5.20544 Å for c, respectively.[28] Recent investigations from cation-doped ZnO indicate that the distance of doping atoms can influence the calculated results due to the interaction of doping atoms.[29] To weaken the interaction in Cu–Cu configuration, the separation distance is as large as possible. Then, the $Zn_{1-x}Cu_xO$ system is optimised with the lattice constants and the

positions of substitutional atoms. In the optimisation process, the energy change, maximum force, maximum stress, and maximum displacement tolerances are set to 2×10^{-5} eV/atom, 0.05 eV/Å, 0.1 GPa, and 0.002 Å, respectively. In addition, both lattice constants and atomic positions are optimised whenever available. Furthermore, the scissor operation has been used to obtain the exact optical absorption spectra in the low energy range in the optical absorption of ZnO and the ZnCuO alloys.

Table 1. Lattice constants and final energy of intrinsic ZnO at different cut-off energies.

cut-off energy $E_{\rm out}$/ eV		400	420	440	460	480	500
lattice constants / Å	a	3.435628	3.296271	3.270632	3.254022	3.253909	3.253838
	c	5.36892	5.38986	5.262189	5.222463	5.221384	5.22379
final energy/eV		–3434.81	–3435.47	–3435.72	–3435.80	–3435.95	–3436.10

3. Results and discussions

3.1. The optimisation of the structure of ZnCuO

We first calculate the structural parameter of pure wurtzite ZnO with $a = b = 3.24927$ Å, $c = 5.20544$ Å. Then, we obtaine these optimised data given in Table 2. These data are in agreement with experimental and other theoretical results.

When the Zn atom is substituted by the Cu atom, the lattice constant and the local atomic positions are changed, but the shape of the wurtzite structure is unchanged. Because of the reduced bond length of the Cu–O bond, the c-axis lattice constant decreases with the increase of copper concentration as shown in Fig. 2.

Table 2. Lattice constants of intrinsic ZnO.

	a/ Å	c/ Å	c/a
our work	3.254	5.222	1.604
Ref. [30]	3.258	5.220	1.602
Ref. [31]	3.280	5.297	1.615
Ref. [32]	3.292	5.292	1.608

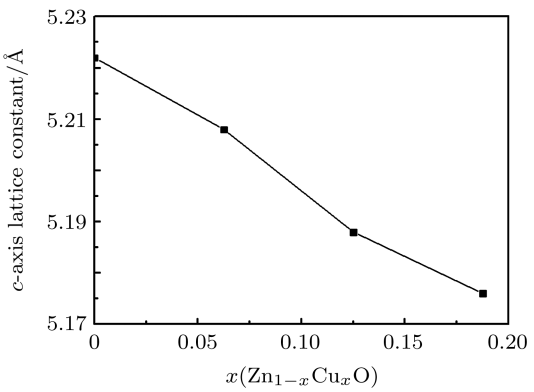


Fig. 2. The c-axis lattice constant of pure ZnO and $Zn_{1-x}Cu_xO$ alloys.

3.2. Electronic properties

Figure 3(a) shows the energy band structure of pure ZnO. The direct band gap is about 0.5 eV at a highly symmetric G point, which is close to the earlier simulations.[33,34] The underestimated band gap can be attributed to the choice of exchange–correlation energy within the CASTEP simulation module. Although the band gap calculated in the local density approximation (LDA) or GGA is about 0.5–1.0 eV and the band gap calculated in GGA is always less than that of LDA, it does not have an impact on the optical property analysis and the aberration can be compensated by the scissors approximation.

Figure 3(b) depicts that the valence band (VB) mainly consists of the 2p, 2s states of O and 3d states of Zn. In the uppermost valence band, O 2p states are predominantly found between –6.9 and 0 eV, while the O 2s states appear in the range of –17.8 – –15.8 eV. It can be observed that Zn 3d states give rise to some bands in the energy range of –7 – –4.5 eV below the valence band maximum (VBM), which shows a rapid and wave-vector dispersion outside G. Besides, the lowest conduction band (CB) is dominated by Zn 4s states, and the CB is primarily derived from O 2p and Zn 4s states.

In Figs. 4 and 5, we can see that, except Zn 3d states and O 2p states, the Cu 3d states contribute a lot to the upper VB in $Zn_{0.9375}Cu_{0.0625}O$. Moreover, the energy levels of Cu 3d states within the valance band overshoot the Fermi level. Compared to Fig. 4(b), Fig. 5(b) shows that the 3d states of Zn cause the peak located between –7 and –4.5 eV in the VB to shift toward lower energies in the energy range of –8.5 – –6 eV obviously, which is caused by the 2p states of oxygen atoms bonded to Cu atoms. There-

fore, a new peak located between –7 and –4 eV in the VB appears. Meanwhile, from Figs. 4(a) and 5(a), we can conclude that strong localisation of the 2s states of O bonded to Cu atoms causes the peak located between –18 and –16 eV in the VB to shift toward lower energies.

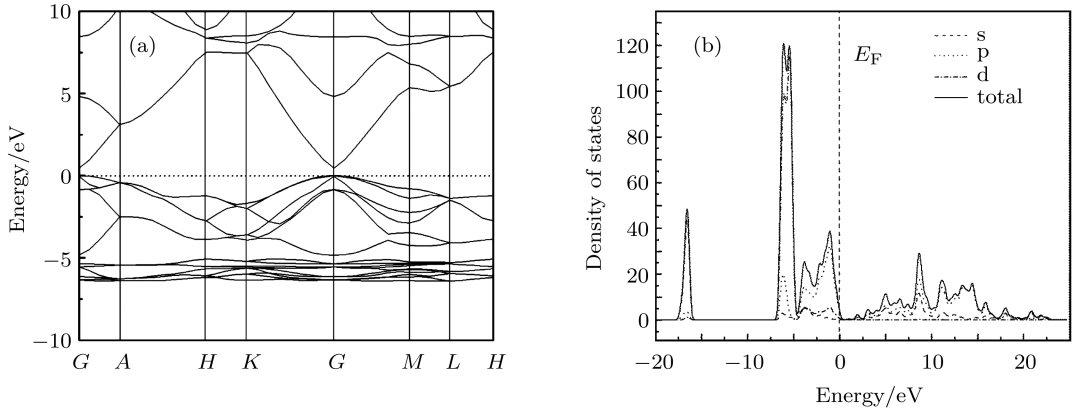


Fig. 3. (a) The energy band structure and (b) density of states (DOS) of pure ZnO.

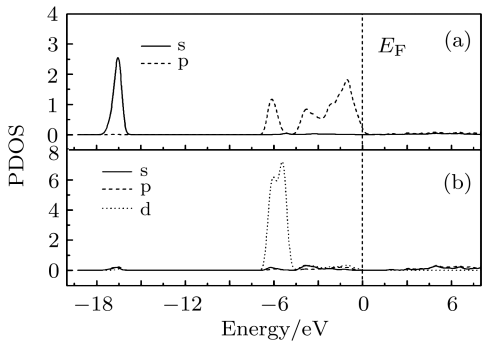


Fig. 4. (a) The partial density of states (PDOS) of an O atom in intrinsic ZnO. (b) The PDOS of a Zn atom in intrinsic ZnO.

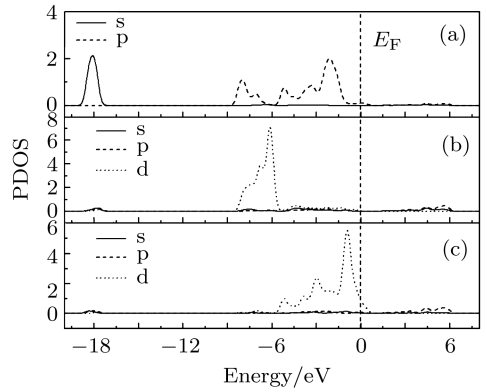


Fig. 5. The PDOS of an O atom (a), a Zn atom (b) and a Cu atom (c) in $Zn_{0.9375}Cu_{0.0625}O$.

Figure 6 reveals that the large hybridisation of the Cu 3d states with the O 2p states is the magnified spectrum in the energy range of –4 – 1 eV. Simultaneously, it is necessary to point out that the hybridisation is not the same in ZnCuO alloy as that in pure ZnO. From Figs. 4 and 6, we find that in the uppermost valence band, the hybridisation is determined between the Zn 3d and O 2p states in pure ZnO, and in ZnCuO alloy and that it comes from the Cu 3d and O 2p states.

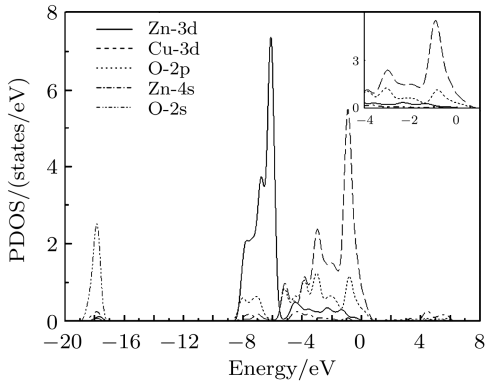


Fig. 6. The PDOS of ZnO doped with 6.25% of Cu. Fermi level is set to be zero.

Figure 7 shows the density of states in the $Zn_{1-x}Cu_xO$ system. When Cu is doped, the PDOS of O 2s states shifts to the lower energy compared to the pure ZnO in Fig. 7(a), which mainly comes from the strong localisation between 2s states of O atoms and Cu atoms. A shift of Zn 3d states to the lower energy creates a new peak between –7 and –8.7 eV in the VB, which is caused by the 2p states of O atoms bonded to Cu atoms. Besides, both O 2p and Cu 3d states become more delocalised in the top of the valence band with a narrower bandwidth as the Cu concentration increases. As a result, the excitons will be effectively

localised in the ZnCuO alloy, which can influence its band edge emission.

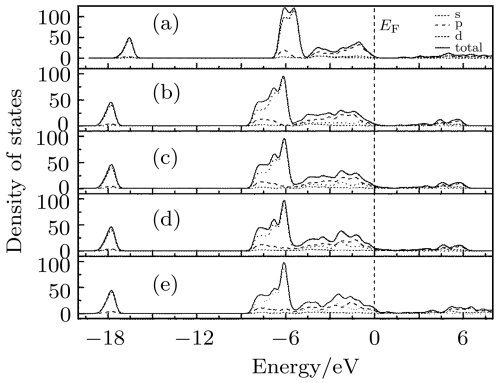


Fig. 7. The PDOS and TDOS of $Zn_{1-x}Cu_xO$. (a) $x = 0$, (b) $x = 0.0625$, (c) $x = 0.125$, (d) $x = 0.1875$, and (e) $x = 0.25$.

In general, the band gap of the ZnCuO alloy is narrower than that of pure ZnO. It confirms that the Cu incorporation into ZnO can induce the obvious band gap narrowing. In our simulation, the energy band gap will disappear completely when 25% concentration of Cu is doped in the supercell ZnO model. In the upper part of the valance band, when x varies from 0.0625 to 0.25, the valance band shifts to the higher energy range. Moreover, this shift can lead to the obvious variation of electronic properties. On the other hand, the CB of ZnO doped with Cu shows a slight shift to the lower energy due to the incorporation of Cu 4s electrons. Therefore, the band gap of ZnO doped with Cu is lower than the E_g of intrinsic ZnO. It is noticeable that the variations of band gap are not obvious in a high concentration ($> 18.75\%$), and it may indicate that the modulation of the band gap by Cu substitution is limited. This result is in qualitative agreement with the experimental data. Ahn *et al.*[12] reported that the band gap of ZnO can be reduced by 0.21 eV at low Cu composition ($x \sim 10\%$).

3.3. Optical properties

To investigate the optical properties of the Cu-doped ZnO system, it is necessary to calculate the imaginary part of the dielectric function $\varepsilon_2(\omega)$. It is known that the interaction of a photon with the electron can be described in terms of time-dependent perturbations in the ground-state electronic states. Optical transitions between occupied and unoccupied states are caused by the electric field of the photon. The spectra arising from the excited states can be described as a joint density of states between the valence and conduction bands. The function $\varepsilon_2(\omega)$ can be calculated straightforwardly using the momentum matrix elements which are given by the eigenvectors obtained as the solution of the corresponding Schrödinger equation. Evaluating these matrix elements, we use the corresponding eigenfunctions of each of the occupied and unoccupied states. And the real part $\varepsilon_1(\omega)$ of dielectric function can be evaluated from imaginary part $\varepsilon_2(\omega)$ by Kramer–Kronig relationship. All the other optical constants can be derived from $\varepsilon_1(\omega)$ and $\varepsilon_2(\omega)$, such as reflectivity $R(\omega)$, absorption coefficient $\alpha(\omega)$, refractive index $n(\omega)$, and energy-loss spectrum $L(\omega)$[34]

$$R(\omega) = \left| \frac{\sqrt{\varepsilon_1(\omega) + \mathrm{j}\varepsilon_2(\omega)} - 1}{\sqrt{\varepsilon_1(\omega) + \mathrm{j}\varepsilon_2(\omega)} + 1} \right|, \quad (1)$$

$$\alpha(\omega) = \sqrt{2}\omega \left[\sqrt{\varepsilon_1^2(\omega) + \varepsilon_2^2(\omega)} - \varepsilon_1(\omega) \right]^{1/2}, \quad (2)$$

$$n(\omega) = \left[\sqrt{\varepsilon_1^2(\omega) + \varepsilon_2^2(\omega)} + \varepsilon_1(\omega) \right]^{1/2} \Big/ \sqrt{2}, \quad (3)$$

$$L(\omega) = \varepsilon_2(\omega) / \left[\varepsilon_1^2(\omega) + \varepsilon_2^2(\omega) \right]. \quad (4)$$

Since $\varepsilon_2(\omega)$ is the core of the optical properties for any materials, Fig. 8 shows its dependence on the photon energy for pure ZnO and the ZnCuO alloy. For pure ZnO, there are three main peaks in $\varepsilon_2(\omega)$, at 1.13, 5.99, and 10.6 eV. The peak at around 1.13 eV should mainly be caused by optical transitions between O 2p states in the highest valence band and Zn 4s states in the lowest conduction band, which is very close to the other evaluations,[34] and it is not far from the direct band gap of 0.5 eV. The peak at about 5.99 eV is from the optical transition between the Zn 3d and O 2p states, and the weak peak at 10.6 eV is mainly derived from the optical transition between the Zn 3d and O 2s states. For the ZnCuO alloy, the first peak is significantly shifted toward low energies while the second and third peaks show a blue shift. It is noticeable that the optical transitions between the Zn 4s and O 2p states are at 0.627, 0.470, 0.376 and 0.318 eV, which correspond to the different Cu concentrations ranging from $x = 6.25\%$ to 25%. And, the probability of the electron transfer from the O 2p states in the highest VB to the Zn 4s states in the lowest CB is higher when ZnO is doped with Cu. The shift of the optical transition indicates that the direct band gap decreases, which is in good agreement with the result of DOS. Besides, the optical transition has been gradually enhanced with increasing Cu concen-

trations, which induces the enhancement of the band edge emission of the ZnCuO alloy.

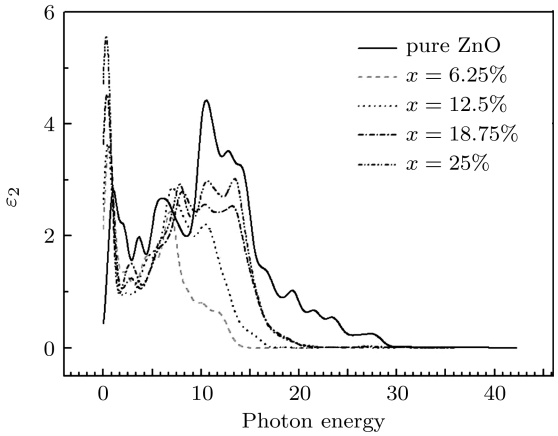


Fig. 8. The imaginary part of the dielectric function $\varepsilon_2(\omega)$ of pure ZnO and $Zn_{1-x}Cu_xO$ alloy.

Figure 9 illustrates the optical absorption spectra of the $Zn_{1-x}Cu_xO$ system under the scissor operation in the range of 0–5 eV. Due to the underestimation of the band gap, it is difficult to obtain the exact optical band gap. In our calculations, we have used the energy scissor approximation for 2.7 eV to fit the absorption edge of the experimental value. This method is effective for a variety of systems.[35−37] It is clearly observed that the Cu incorporation induces the redshift of the optical absorption edge.

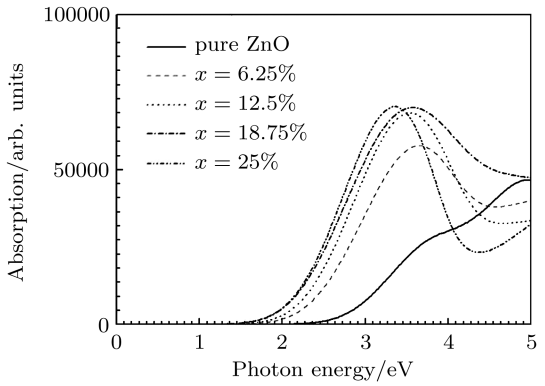


Fig. 9. Optical absorption spectra $\alpha(\omega)$ of pure ZnO and $Zn_{1-x}Cu_xO$ alloy.

The reflectivity $R(\omega)$, refractive index $n(\omega)$, and electron energy loss spectrum $L(\omega)$ as functions of the photon energy for pure ZnO and $Zn_{0.75}Cu_{0.25}O$ alloy are shown in Figs. 10–12, respectively. The refractive index and reflectivity of Cu-doped ZnO enhance sharply in the low energy range as compared to those of the pure ZnO, which indicates that the band gap of Cu-doped ZnO decreases. We also observe the peaks between 20 and 25 eV in the energy loss spectra $L(\omega)$ which is also an important factor describing the energy loss of a fast electron traversing in a material. The peaks in $L(\omega)$ spectra represent the characteristic associated with the plasma resonance, and the corresponding frequency is the so-called plasma frequency, above which the material exhibits the dielectric behaviour $[\varepsilon_1(\omega) > 0]$ while below which the material behaves the metallic property $[\varepsilon_1(\omega) < 0]$. That is to say, the positions of peaks in $L(\omega)$ spectra indicate the point of transition from the metallic property to the dielectric property for a material. In addition, the peaks of $L(\omega)$ also correspond to the trailing edges in the reflection spectra, for instance, the peak of $L(\omega)$ for $Zn_{0.75}Cu_{0.25}O$ alloy is at around 21 eV corresponding to the abrupt reduction of $R(\omega)$.

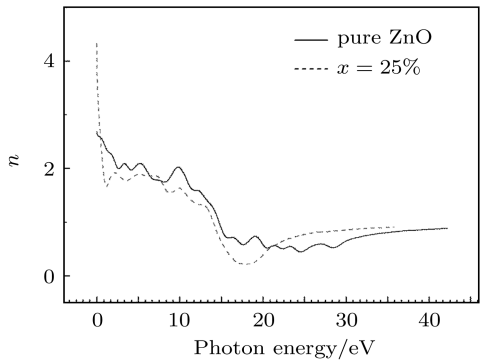


Fig. 10. Refractive index $n(\omega)$ of pure ZnO and $Zn_{0.75}Cu_{0.25}O$ alloy.

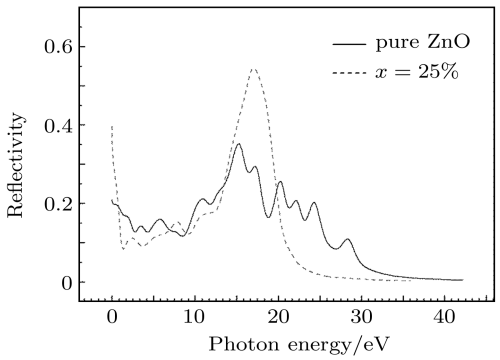


Fig. 11. Reflectivity $R(\omega)$ of pure ZnO and $Zn_{0.75}Cu_{0.25}O$ alloy.

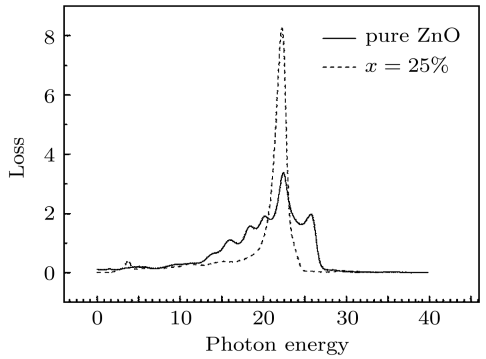


Fig. 12. Loss function $L(\omega)$ of pure ZnO and $Zn_{0.75}Cu_{0.25}O$ alloy.

4. Conclusion

In summary, a first-principles study has been performed to evaluate the electronic and optical properties of the $Zn_{1-x}Cu_xO$ system. Increasing Cu concentration can induce the band gap narrowing. Subsequently, optical transition between the uppermost valence band and the lowest conduction band has shifted to the low energy range with increasing Cu concentration. Besides, most important optical constants such as the dielectric function, reflectivity, refractive index, and electron energy loss function also experience significant changes when ZnO is doped with Cu. In particular, the optical absorption edge of ZnO doped with Cu shows a redshift. The computed DOS of Zn and Cu under different doping conditions enables a simple explanation of this phenomenon based on electron transfer mechanism.

References

[1] Lorenz M, Kaidashev E M, Rahm A, Nobis T, Lenzner J, Wagner G, Spemann D, Hochmuth H and Grundmann M 2005 *Appl. Phys. Lett.* **86** 143113

[2] Hsu H C, Wu C Y, Cheng H M and Hsieh W F 2006 *Appl. Phys. Lett.* **89** 013101

[3] Chen D H, Guo J, Huang D, Li G X and Shao Y Z 2008 *Acta Phys. Sin.* **57** 1078 (in Chinese)

[4] Bi Y J, Dong Y C, Guo Z Y, Lin Z and Sun H Q 2008 *Acta Phys. Sin.* **57** 7800 (in Chinese)

[5] Cox S F J, Davis E A, Cottrell S P, King P J C, Lord J S, Gil J M, Alberto H V, Vilao R C, Duarte J P, Ayres de Campos N, Weidinger A, Lichti R L and Irvine S J C 2000 *Phys. Rev. Lett.* **86** 2601

[6] van de Walle C G 2000 *Phys. Rev. Lett.* **85** 1012

[7] Kohan A F, Ceder G, Morgan D and van de Walle C G 2000 *Phys. Rev.* B **61** 15019

[8] Zhang S B, Wei S H and Zunger A 2001 *Phys. Rev.* B **63** 075205

[9] Cai Y R, Ding R X, Shi L C, Song J X, Wu J and Yang Y T 2008 *Acta Phys. Sin.* **57** 7151 (in Chinese)

[10] Zhang X D, Guo M L, Li W X and Liu C L 2008 *J. Appl. Phys.* **103** 063721

[11] Qiu D J, Feng C M, Feng A M and Wu H Z 2008 *Chin. Phys.* B **17** 0690

[12] Ahn K S, Deutsch T, Yan Y F, Jiang C S, Perkins C L, Turner J and Mowafak A J 2007 *J. Appl. Phys.* **102** 023517

[13] Xiong Z H and Jiang F Y 2007 *J. Phys. Chem. Solids* **68** 1500

[14] Chen Q Y, Dong C J, Duan M Y, Hu Z G, Xu M and Zhou H P 2008 *Chin. Phys.* B **17** 6520

[15] Lin S S, Lu J G, Ye Z Z, He H P, Gu X Q, Chen L X, Huang J Y and Zhao B H 2008 *Solid State Commun.* **148** 25

[16] Thomas M A and Cui J B 2009 *J. Appl. Phys.* **105** 093533

[17] Samanta K, Bhattacharya P and Katiyar R S 2009 *J. Appl. Phys.* **105** 113929

[18] Ando K, Saito H, Jin Z, Fukumura T, Kawaski M, Matsumoto Y and Koinuma H 2001 *J. Appl. Phys.* **89** 7284

[19] Buchholz D B, Chang R P H, Song J H and Kettersom J B 2005 *Appl. Phys. Lett.* **87** 082504

[20] Ye L H, Freeman A J and Delley B 2006 *Phys. Rev.* B **73** 033203

[21] Park M S and Min B I 2003 *Phys. Rev.* B **68** 224436

[22] Charkraborti D, Narayan J and Prater J T 2007 *Appl. Phys. Lett.* **90** 062504

[23] Perdew J P, Burke K and Ernzerhof M 1996 *Phys. Rev. Lett.* **77** 3865

[24] Payne M C, Teter M P, Allan D C, Arias T A and Joannopoulos J D 1992 *Rev. Mod. Phys.* **64** 1045

[25] Hamann D R, Schlüter M and Chiang C 1979 *Phys. Rev. Lett.* **43** 1494

[26] Sun J, Zhou X F, Fan Y X, Chen J, Wang H T, Guo X, He J and Tian Y 2006 *Phys. Rev.* B **73** 045108

[27] Monkhorst H J and Pack J D 1976 *Phys. Rev.* B **13** 5188

[28] Wyckoff R W G 1982 *Crystal Structures* 2nd ed. (Malabar, FL: Krieger) Vol. 1

[29] Huang L M, Rosa A L and Ahuja R 2006 *Phys. Rev.* B **74** 075206

[30] Tang X, Lü H F, Ma C Y, Zhao J J and Zhang Q Y 2008 *Acta Phys. Sin.* **57** 1066 (in Chinese)

[31] Decremps F, Datchi F, Saitta A M and Polian A 2003 *Phys. Rev.* B **68** 104101

[32] Jaffe J E, Snyder J A, Lin Z J and Hess A C 2000 *Phys. Rev.* B **62** 1660

[33] Zhang X D, Guo M L, Li W X and Liu C L 2008 *J. Appl. Phys.* **103** 063721

[34] Sun J, Wang H T, He J and Tian Y 2005 *Phys. Rev.* B **71** 125132

[35] Li J, Wei S H, Li S H and Xia J B 2006 *Phys. Rev.* B **74** 081201

[36] Zhang X D, Guo M L, Li W X and Liu C L 2008 *J. Appl. Phys.* **103** 063721

[37] Xu M, Zhao H, K. Ostrikov, Duan M Y and Xu L X 2009 *J. Appl. Phys.* **105** 043708